Research article

Adsorptive stripping voltammetric determination of Tetracycline in pharmaceutical capsule formulation using Poly(Malachite green) modified glassy carbon electrode

Mahilet Turbale [a], Amsalu Moges [b], Mulugeta Dawit [c], Meareg Amare [d],[*]

[a] Samara University, Ethiopia
[b] Debre Markos University, Ethiopia
[c] Debre Tabor University, Ethiopia
[d] Bahir Dar University, Ethiopia

ARTICLE INFO

ABSTRACT

A selective and sensitive electrochemical method based on glassy carbon electrode modified with poly(malachite green) was developed for determination of tetracycline in pharmaceutical capsule formulation. Cyclic voltammetry and electrochemical impedance spectroscopy using $[Fe(CN)_6]^{3-/4-}$ as a probe were used to characterize the potentiodynamiclly deposited poly(malachite green) on the surface of glassy carbon electrode. In contrast to the unmodified glassy carbon electrode, the fabricated poly(malachite green) modified glassy carbon electrode showed catalytic property towards two steps irreversible oxidation of tetracycline. Better correlation of the oxidative peak current with the scan rate than with the square root of scan rate supported by slope of 0.60 for log(current) versus log(scan rate) indicated that the oxidation reaction of tetracycline at the modified electrode was predominantly controlled by electron exchange step at the solution polymer interface. Under optimized solution pH, and accumulation parameters, the square wave adsorptive anodic striping peak current response of the modified electrode showed linear dependence on concentration of tetracycline in the range 5–100 μM with determination coefficient, method detection limit, and quantification limit of 0.99588, 1.6 μM, and 5.3 μM, respectively. The tetracycline content of a capsule sample claimed to have 250 mg/capsule was found to be 250.53 mg/capsule with 0.21% deviation. Excellent spike recovery result of 99.80%, and 98.49–99.78% recovery of tetracycline in capsule sample in the presence of 50–200% of UA, AA, and ampicillin validated the applicability of the method for determination of tetracycline in real samples with complex matrix like capsule formulations.

1. Introduction

Tetracyclines constitute a family of well-known broad-spectrum antibiotics routinely used for prevention and control of diseases in human and veterinary medicine. They inhibit bacteria's protein synthesis by blocking ribosome action against the linking of aminoacil-tRNA's and destroy bacterial cellular membrane [1]. Moreover, they also find wide applications as a feed additive for cattle breeding; as an alternative drug for people allergic to penicillin; and in the control of plant diseases [1]. In human medicine, tetracycline antibiotics also have been used for the treatment of different types of infections, including respiratory tract infections, urethritis and severe acene [2]. In the past decade, tetracyclines have been the drug of choice for treatment of malaria due plasmodium falciparum [3]. Because of their board spectrum activity and low

production cost; the four tetracyclines (tetracycline, chlortetracycline, oxytetracycline, and doxycycline) are commonly used in food protection animals including honeybee [4].

Tetracycline (TC) can adsorb strongly onto environmental materials, where it still keeps its activity [5]. TC (Figure 1), which has significant effect on gram-positive and gram-negative bacteria, is widely used as an important antibiotic to control bacterial infections in both animal models and clinical studies [6, 7]. This antibiotic molecule is found in some food products, such as milk [8] and egg [9]. In spite of its use for prevention and control of many bacterial diseases, tetracycline has gastrointestinal side effects, nausea, vomiting, and diarrhea [10]. It is known as a hepatotoxic C agent in pregnant women leading to serious threat to human health [11, 12]. Various studies indicated that even low-level dose of TC for long period could show bacteria resistance [13] necessitating
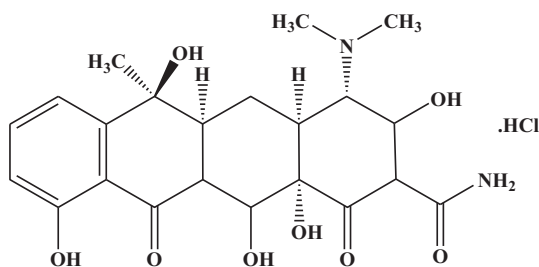

Figure 1. The chemical structure of tetracycline hydrochloride.

continuous monitoring of its level in different samples including pharmaceutical formulations.

Microbiological method [14], high–performance liquid chromatographic method (HPLC) with different detectors [15, 16, 17, 18], have been reported for determination of tetracycline in real samples. Although these methods are known of their sensitivity and accuracy, their high cost and complicated operation procedure limited their extensive application [19]. Therefore, the need to develop a sensitive, accurate, less expensive and easy operation method for determination of TC in different samples is still important.

Electrochemical methods, which are simple, fast, sensitive, inexpensive, environmentally friendly, have been known as potential methods for tetracycline determination [19]. Voltammetric methods using carbon-based electrodes modified with various materials [5, 20, 21, 22, 23, 24, 25, 26] have been reported for determination of TC in real samples. Most of the reported electrode surface modifiers are not readily available, are expensive, and the modification seem to be time taking. Thus, development of an alternative sensitive, selective and accurate electrochemical method using easily available surface modifiers is crucial.

Recently, numerous conjugated polymers (intrinsically conducting polymers) including malachite green have been electrochemically synthesized for chemical and biochemical sensors applications [27, 29]. Poly(malachite green) modified electrochemical sensors have been reported to exhibit interesting enhancement in the electrocatalytic activity towards the oxidation or reduction of selected electroactive species [29, 30, 31].

To the best of our knowledge, poly(malachite green) modified glassy carbon electrode has not been reported for determination of TC in pharmaceutical capsule sample. The aim of this work was thus to develop a sensitive, selective, and accurate stripping voltammetric method based on poly(malachite green) modified glassy carbon electrode (PMG/GCE) for determination of tetracycline in pharmaceutical capsule formulation.

2. Experimental part

2.1. Chemicals and reagents

Tetracycline (99.81%, sigma Aldrich, USA), malachite green (Himedia Laboratories Pvt. Ltd), ethanol (97%, Fine Chemical General Trading, Addis Ababa, Ethiopia), sulfuric acid (98%) and hydrochloric acid (35.4%) both from Loba Chemie Pvt.Ltd, disodium hydrogen phosphate (99%) and sodium dihydrogen phosphate (97%) both from Sisco Research Laboratories Pvt.Ltd, ascorbic acid (99%) and sodium hydroxide (97%) both from Blulux Laboratories Ltd were used. All chemicals were of analytical grade that they were used without further purification. Distilled water was used throughout the experiment.

2.2. Apparatus

Electrochemical experiments were conducted using CHI760E electrochemical workstation (CH Instruments, Austin, USA) with a

conventional three-electrode system at room temperature. PMG/GCE or bare glassy carbon electrode, platinum coil, and Ag/AgCl (3 M KCl) were employed as working, auxiliary, and reference electrode, respectively. The pH meter (Adwa model AD800), electronic balance (Denver Instrument), and refrigerator were used to adjust the pH of solution, measure mass, and preserve samples, respectively.

2.3. Fabrication of PMG/GCE

PMG film was deposited on the surface of glassy carbon electrode following reported procedure with minor modification [28]. Briefly: prior to electropolymerization, the surface of glassy carbon electrode was polished consecutively with alumina slurries of different course sizes (1.0, 0.3, and 0.05 μm) to a mirror like surface. Electropolymerization of malachite green on the surface of the polished GCE was conducted by scanning the potential of the GCE in 10 mM malachite green monomer dissolved in pH 6 PBS containing 0.5 M $NaNO_3$ between -1.4 to 1.8 V at a scan rate of 0.1 V s^{-1} for 10 cycles. After rinsing the electrode copiously with distilled water, and scanning in monomer free 0.5 M sulfuric acid between -0.8 to +0.8 V until steady voltammogram was obtained, the fabricated PMG/GCE was ready for use.

2.4. Standard preparation

The phosphate buffer solution (PBS) was prepared by mixing equimolar (0.1 M) of NaH_2PO_4 and Na_2HPO_4 the pH of which was adjusted by adding 0.1 M NaOH or HCl. Tetracycline stock solution (1 mM) was prepared by dissolving 0.024 g in 50 mL of volumetric flask with ethanol. The working solution (0.1 mM) and the various calibration standard solutions of TC were prepared from the stock solution through serial dilution with PBS of the appropriate pH.

2.5. Real sample preparation

Tetracycline capsule sample was prepared following the reported procedure [1] with minor modification. Briefly: TC capsules (EPHARM brand) with a nominal content of 250 mg/capsule were purchased from a pharmacy in Bahir Dar city, Ethiopia. The powder collected from five randomly selected capsules was weighed to acquire the mean mass and then homogenized using a mortar and pestle. Capsule stock solution was prepared by dissolving an appropriate amount of the powder (about 30 mg) in ethanol to a final volume of 100 mL. After filtering for removing insoluble particles, nominal 56.98 μM capsule sample solution was prepared from the capsule stock solution using PBS pH 7.5 for determination, recovery and interference studies.

3. Results and Discussion

3.1. Fabrication and characterization of PMG/GCE

Cyclic voltammograms of glassy carbon electrode in pH 6.0 PBS containing malachite green are presented in Figure 2. As can be seen from the figure, the peak current of the cathodic (peak-1) and anodic (peak-2) peaks that appeared at -0.5, and 0.9 V, respectively increased with increasing scan cycles indicating polymer film growth.

Inset of Figure 2 (curves *a* & *b*) depicts the CVs of bare GCE (*a*) and PMG/GCE (*b*) in a monomer free 0.5 M of H_2SO_4 solution. While peak-1 (curve a) at -0.6 V and peak-1' (curve b) at -0.4 V are assigned to reduction of molecular oxygen at the unmodified and modified GCE, respectively, couple of redox peaks (peak-2 & peak-2'), which are distinct to the PMG/GCE, indicated deposition of a redox active polymer film at the surface of the GCE. The observed lower oxygen reduction potential (-0.4 V) at the PMG/GCE relative to its value at the unmodified GCE (-0.6 V) is clear indication of catalytic behavior of the modified surface of the electrode and hence PMG polymer film.
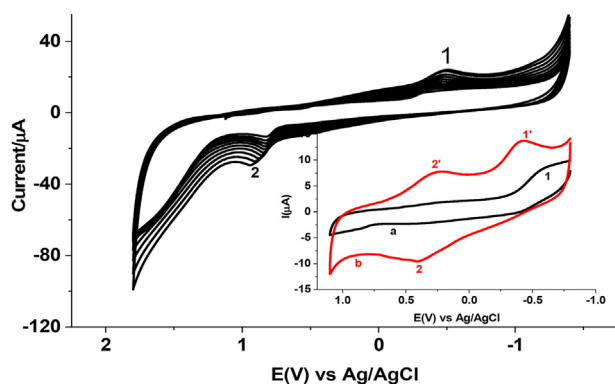
Figure 2. CVs of GCE in pH 6.0 PBS containing 10 mM malachite green and 0.5 M $NaNO_3$ scanned between -1.4 and 1.8 V for 10 cycles at a scan rate of 0.1 V s^{-1}. Inset: CVs of (a) bare GCE, and (b) stabilized PMG/GCE in monomer free 0.5 M H_2SO_4 scanned between -0.8 and 1.1 V at scan rate of 0.1 V s^{-1}.

3.2. Characterization of PMG/GCE

The modified electrode was characterized by two techniques; cyclic voltammetry and electrochemical impedance spectroscopy using $[Fe(CN)_6]^{3-/4-}$ as a probe.

3.2.1. Cyclic voltammetric characterization

Cyclic voltammetry using $[Fe(CN)_6]^{3-/4-}$ as a probe was used to characterize the poly(malachite green) modified glassy carbon electrode (Figure 3). Appearance of couple of redox peaks in opposite scan directions at both electrodes with comparable peak current but with lower peak-peak separation at the PMG/GCE (ΔE 170 mV) than at the unmodified electrode (ΔE 337 mV) indicated catalytic property of the PMG/GCE towards the $Fe^{3+} \Leftrightarrow Fe^{2+}$ reaction and hence confirming the surface modification of the electrode.

3.2.2. EIS characterization

Electrochemical impedance spectroscopy (EIS) data enables to evaluate the electrical nature of the electrode surface including the double layer capacitance, charge transfer resistance, solution resistance and hence nature of the modifier. Nyquist plots of the unmodified (a) and modified (b) glassy carbon electrodes are presented in Figure 4. As can be seen from the figure, both electrodes exhibited combination of semicircle of different diameters at high frequency region and linear line at low frequencies. The semicircle portion at higher frequencies corresponds to the electron transfer limited process, and the linear portion at lower frequencies corresponds to the diffusion process [32].
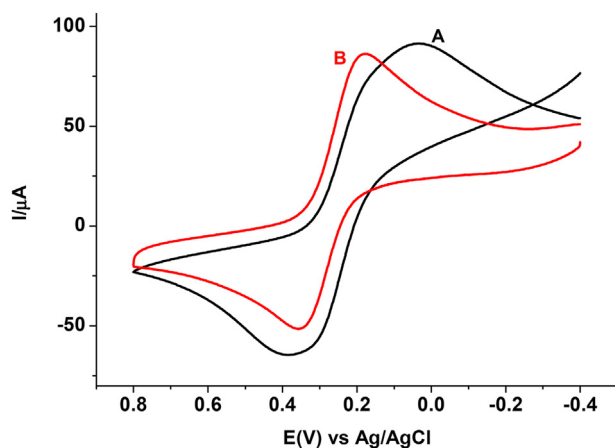

Figure 3. CVs of (A) unmodified GCE and (B) PMG/GCE in pH 7.0 PBS containing 10 mM $[Fe(CN)_6]^{3-/4-}$) and 0.1 M KCl at scan rate of 0.1 V s^{-1}.
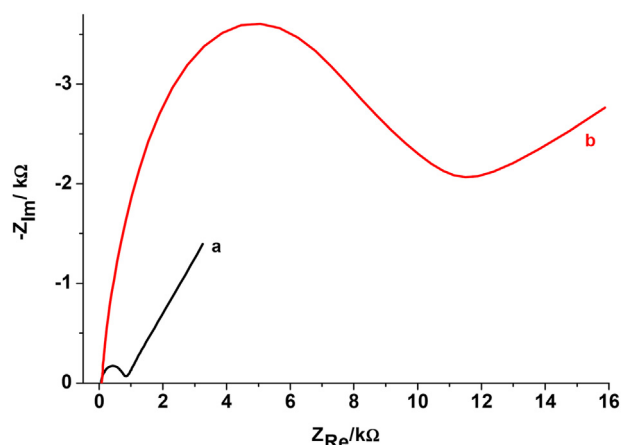

Figure 4. Nyquist plots of the (a) unmodified GCE and (b) PMG/GCE in pH 7.0 PBS containing 10 mM $[Fe(CN)_6]^{3-/4-}$ and 0.1 M KCl at frequency range 0.01–100,000 Hz, applied potential +0.23 V, and amplitude 0.01 V.

The parameters R_s, R_{ct} and C_{dl} of the presumed RC-elements for the studied electrodes were obtained (Table 1) from the respective semicircles by taking into account the relationship between the R_{ct} and C_{dl} (Eq. 1).

$$C_{dl} = \frac{1}{2\pi \; R_{ct} f_{max}} \tag{1}$$

where f_{max}, is the frequency (Hz) corresponding to the maximum value of $-Z''$ at the semi-circle, C_{dl} is the double layer capacitance, R_{ct} is the charge transfer resistance given by the diameter of the semi-circle, and R_s is solution resistance given by the x-axis value corresponding to the semi-circle at maximum frequency.

From the charge transfer resistance values of the two electrodes, the catalytic property of the PMG/GCE, which is less conductive than the unmodified GCE, observed towards $Fe^{3+} \Leftrightarrow Fe^{2+}$ in Figure 3, should be accounted for possible increased effective surface area of the modified surface of the electrode.

3.3. Cyclic voltammetric investigation of TC at PMG/GCE

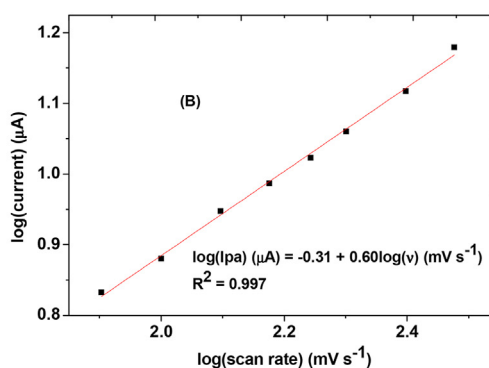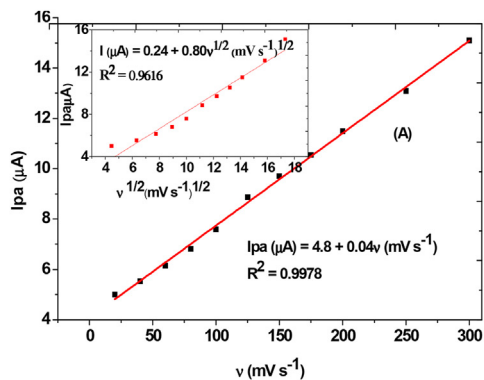#### 3.3.1. Electrochemical behavior of TC at PMG/GCE

Figure 5 shows cyclic voltammograms of bare GCE and PMG/GCE in the absence and presence of 0.1 mM TC in pH 7.0 PBS. While two extremely weak and broad oxidative peaks (a & b) are observed at the unmodified GCE (curve A of Inset), appearance of two well resolved oxidative peaks (a′ & b′) with significantly enhanced peak current at the PMG/GCE (curve B of Inset) showed catalytic property of the polymer modifier towards oxidation of TC. In contrast to the broad peaks (a and b of curve A) centered at 786 and 1023 mV, respectively at the unmodified electrode, appearance of the same peaks (a′ and b′ of curve B) at the modified electrode at much reduced potentials (730 and 924 mV, respectively) could also be taken as supporting evidence for the catalytic property of the modifier towards oxidation of TC.

3.3.2. Effect of scan rate on peak potential and peak current

Cyclic voltammograms of PMG/GCE in pH 7.0 PBS containing TC at various scan rates (20–300 mV s^{-1}) are presented in Figure 6. While observed oxidative peak potential shift in the positive direction for both peaks (a & b) with increasing scan rate confirmed the irreversibility of the oxidation reactions, better correlation of peak current on scan rate (R^2 0.9978) (Figure 7A) than on square root of scan rate (R^2 0.9616) (Inset of Figure 7A) indicated participation of both adsorption and diffusion mass transport with predominantly the adsorption controlled mechanism, which is supplemented by slope of 0.60 (Figure 7B) for plot of *log ip vs log scan rate*.

Table 1. Summary of the calculated RC-circuit elements.

Electrode Type	R_s (Ω)	R_{ct} (kΩ)	C_{dl} (F)
Bare GCE	70	1.0	4.0×10^{-8}
PMG/GCE	70	13	1.2×10^{-6}
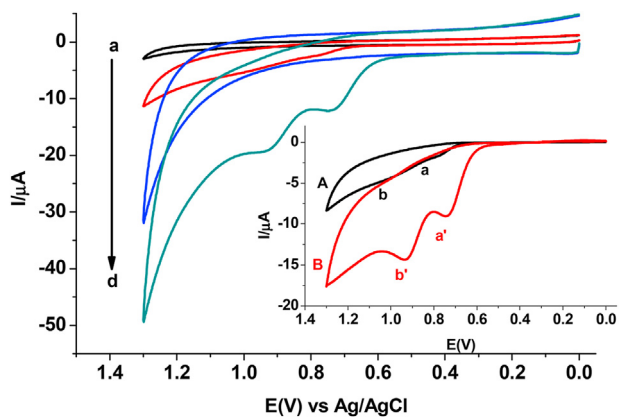
Figure 5. CVs of unmodified GCE (a & b) and PMG/GCE (c & d) in pH 7.0 PBS containing no (a & c) and 0.1 mM TC (b & d) at a scan rate of 0.1 V s⁻¹. Inset: corrected for background current CVs of unmodified GCE (A) and PMG/GCE (B).
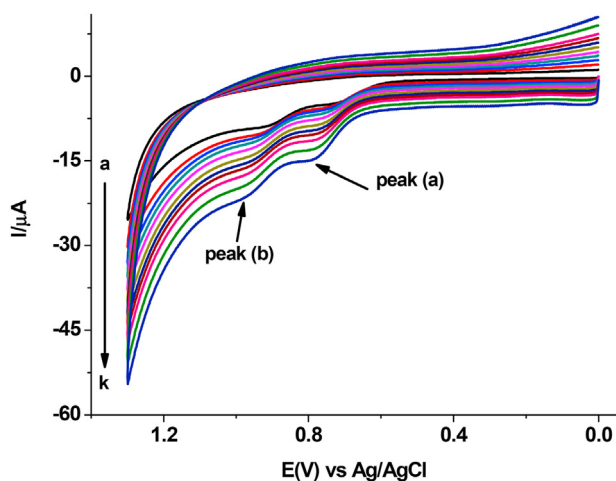
Figure 6. CVs of PMG/GCE in pH 7.0 PBS containing 0.1 mM TC at different scan rates (a–k: 20, 40, 60, 80,100, 125, 150, 175, 200, 250, and 300 mV s⁻¹, respectively).

3.4. SWV investigation of TC at PMG/GCE

The electrochemical oxidation of TC in pH 7.0 PBS was further investigated using two pulse techniques: square wave voltammetry and differential pulse voltammetry. The peak current response of the two techniques for 0.1 mM of TC in pH 7.0 PBS was almost the same (Inset of Figure 8). Thus, for purpose of shortening analysis time, square wave voltammetry was selected for quantification of TC in capsule formulation.

Figure 8 presents corrected for blank square wave voltammograms of 0.1 mM TC in pH 7.0 PBS at unmodified GCE (curve A), and PMG/GCE (curve B). Two oxidative peaks still appear at both electrodes, with nearly threefold enhanced current response at the PMG/GCE showing the sensitivity of the method for TC determination.

3.4.1. Effect of solution pH on peak current and peak potential

Investigation of the effect of pH on the peak parameters (current and potential) is important to predict the possible reaction pathways. Figure 9 shows square wave voltammograms of TC in PBS of pH in the range 5.0–9.0. As can be seen from the figure, both peaks (a & b) showed potential shift in the negative direction with increasing pH indicating participation of protons in the oxidation reactions. The potential shift with pH value for both peaks showed linear dependence on pH in the studied range with slope of 0.059 (peak-a) (curve b of Figure 10) and 0.051 (peak-b) (curve d of Figure 10) showing participation of protons and electrons in exactly 1:1 ratio [2]. In agreement to previously reported works, an oxidation reaction mechanism of TC involving two electrons and two protons (Scheme 1) through the phenolic moiety with the subsequent addition of hydroxyl group was proposed [23].
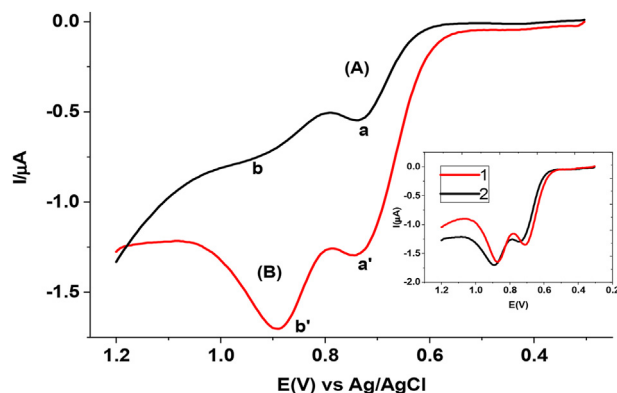
Figure 8. Corrected for blank square wave voltammograms of (A) bare GCE, and (B) PMG/GCE in pH 7.0 PBS containing 0.1 mM TC. Inset: voltammograms of DPV (curve 1) and SWV (curve 2) of PMG/GCE in pH 7.0 PBS containing 0.1 mM of TC.
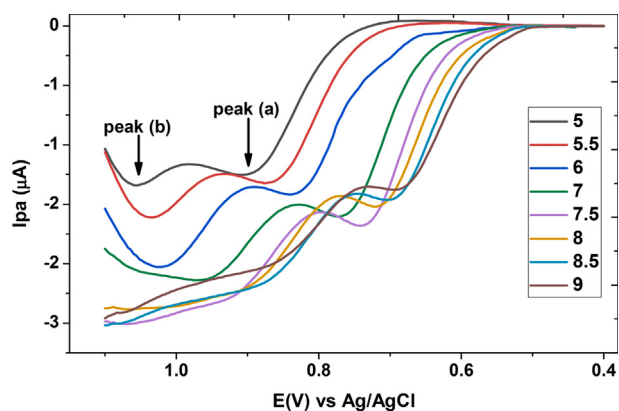

Figure 7. Plot of (A) Ipa *versus* ν, (B) log (Ipa) *versus* $log(\nu)$ of 0.1 mM TC in pH 7.0 PBS at PMG/GCE. Inset: plot of oxidative peak current *versus* square root of scan rate.

Figure 9. Corrected for blank square wave voltammograms of 0.1 mM TC in PBS of various pH values ranging from 5 to 9 at a scan rate of 100 mV s^{-1}.

Although is accompanied with peak shape distortion, peak current for both peaks (curves a & c of Figure 10) increased with pH from 5.0 to 7.5 and then decreased at values beyond 7.5. Comparing the two characteristic peaks of TC, peak (a) that appears at a potential region where capacitive current response of the electrode is minimum was chosen for quantification. Thus, pH 7.5 that gives a well define peak with the highest current was selected for further analysis.

The observed current response trend of the PMG/GCE for TC could be explained considering the pka of TC (pKa 3.3, 7.7 and 9.5) [33] and pka of malachite green (pka 6.9 & 10.3) [34]. As can be seen from curves (a & c of Figure 10), while the increasing trend with pH from pH 5.0 to 7.5 might be ascribed to the electrostatic attraction between the positive charged TC and increasing negative charge density of malachite green, the decreasing current beyond pH 7.5 might be ascribed to repulsive forces between the two.

3.5. Optimization of accumulation parameters

As the rate determining step is found to be predominantly adsorption controlled, optimization of the accumulation potential (E_{acc}) and accumulation time (t_{acc}) is crucial.

3.5.1. E_{acc}

Figure 11 shows the effect of varying the accumulation potential from 450 to 650 mV on the anodic peak current of the two oxidative peaks keeping accumulation time 10 s. As can be observed from the inset, the oxidative current response increased with increasing E_{acc} from 450 to 600 mV after which the resulting peak current was declined. Therefore, E_{acc} of 600 mV was chosen for further experiments.

3.5.2. t_{acc}

Figure 12 presents square wave voltammograms of TC at E_{acc} of 600 mV applied for various length of time. As can been observed from the inset of the figure, the peak current for both peaks increased with increasing the t_{acc} although with different sensitivity. As a compromise between the peak current increment and analysis time, t_{acc} of 20 s was chosen as the optimum value.

3.6. Analytical performance of the method

3.6.1. Variation of peak current with TC concentration

Under the optimized conditions, square wave adsorptive anodic stripping voltammograms (SWAdASVs) were recorded for series of standard solutions of TC (Figure 13). The oxidative peak current response of PMG/GCE for TC showed linear dependence on concentration over the range 5–100 μM (Figure 14) with regression equation, limit of detection ($LoD = 3SD/_m$; n 7), and limit of quantification ($LoQ = 10SD/_m$; n 7) of Ip (μA) = -0.252-0.014C (μM), ($R^2 = 0.994$), 1.6 μM and 2.1 μM, respectively for peak (a) and Ip (μA) = -0.300-0.014C (μM), ($R^2 = 0.996$), 5.4 μM, and 7.02 μM, respectively for peak (b). The same slope for the two regression equations indicated that the sensitivity of the developed method for TC is the same whether peak (a) or peak (b) is considered.

3.7. Determination of level of TC in capsule formulation

The proposed SWAdASV method was used to determine the TC level in EPHARM brand capsule formulation. Peak (a), whose peak shape looks independent of pH and exhibited lower limit of detection, was used in the determination of the level of TC in capsule sample, spike recovery and interference recovery analysis.
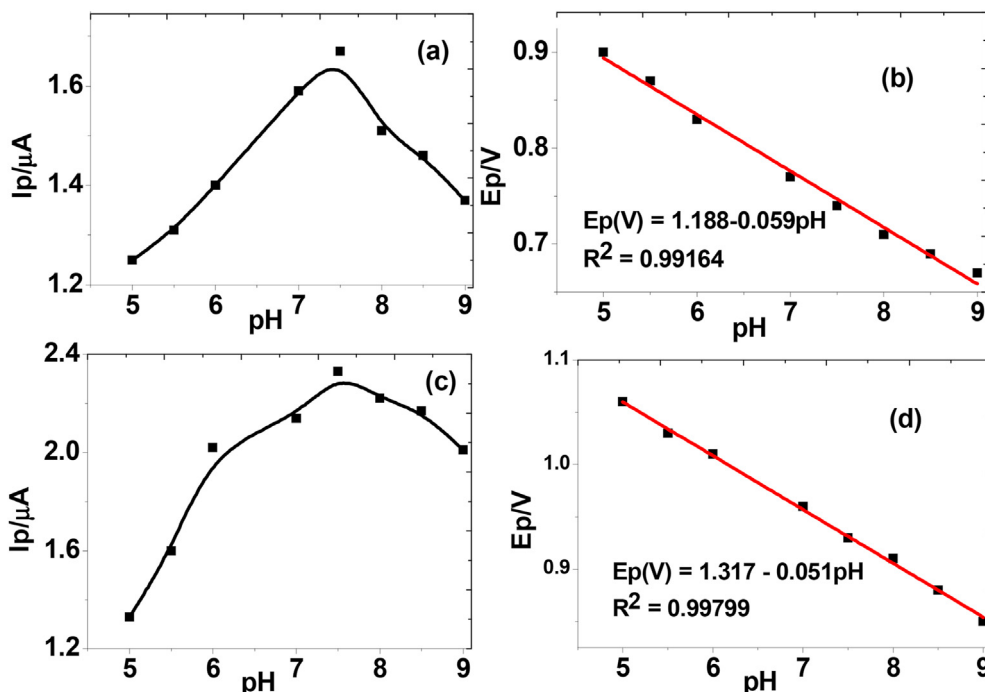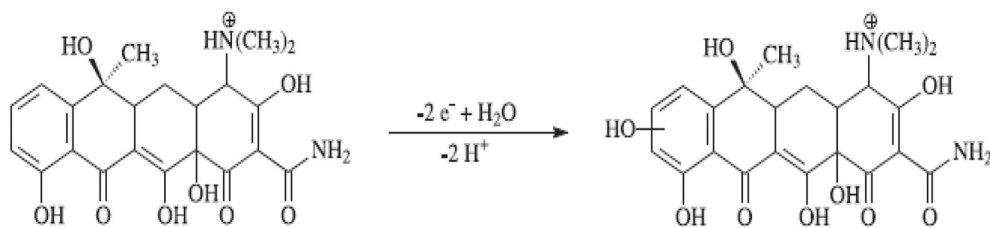

Figure 10. Plot of Ip *vs* pH (curves a & c) and Ep *vs* pH (curves b & d) for peak (a) (curves a & b) and peak (b) (curves c & d), respectively.

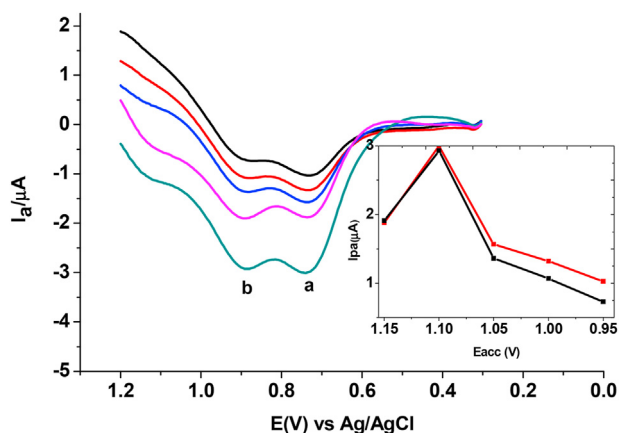**Scheme 1.** Proposed mechanism for oxidation of TC at the PMG/GCE.

Figure 11. SWVs of PMG/GCE in pH 7.5 PBS containing 0.1 mM TC at various E_{acc} (450–650 mV) and t_{acc} 10 s. Inset: plot of Ip vs E_{acc} of 0.1 mM of TC in pH 7.5 PBS.
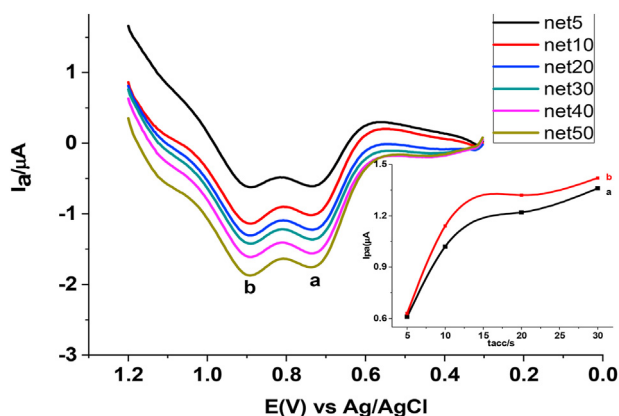

Figure 13. SWAdASVs of pH 7.5 PBS containing various concentrations of TC (a–g: 5, 10, 20, 40, 60, 80, and 100 μM, respectively) at E_{acc} 600 mV, and t_{acc} 20 s.

Figure 12. SWVs of 0.1 mM of TC in pH 7.5 PBS at different t_{acc} (5, 10, 20, 30, 40, and 50 s) and E_{acc} 600 mV. Inset: plot of Ipa vs. t_{acc} for peaks a & b.

Figure 14. Plot of anodic peak current response of PMG/GCE for TC at (a) peak (a), and (b) peak (b) as a function of TC concentration.

Figure 15 presents the SWAdASVs of PMG/GCE in pH 7.5 PBS containing no TP (curve a), the studied capsule sample claimed to have 56.98 μM of TC (curve b), and the same sample solution spiked with 40 μM standard TC (curve c). Inset of Figure 15 presents the voltammograms for the unspiked and spiked capsule sample corrected for the blank. The detected level of TC in the capsule sample solution compared with theoretical level (according to the label), and spike recovery results as calculated using the regression equation for peak (a) are summarized in Table 2. Detection of 57.10 μM of TC in capsule sample claimed to contain 56.98 μM, which is with an error of only 0.21%, indicated the extent of accuracy of the developed method and the capsule preparation.

To validate the reliability of the results, spike recovery and interference recovery analysis were conducted. While spike recovery was conducted for a capsule sample spiked with 40 μM of standard TC (curve 2 of Inset of Figure 15), interference 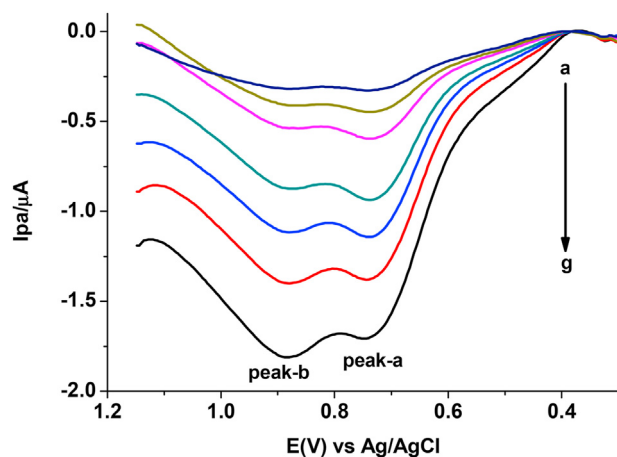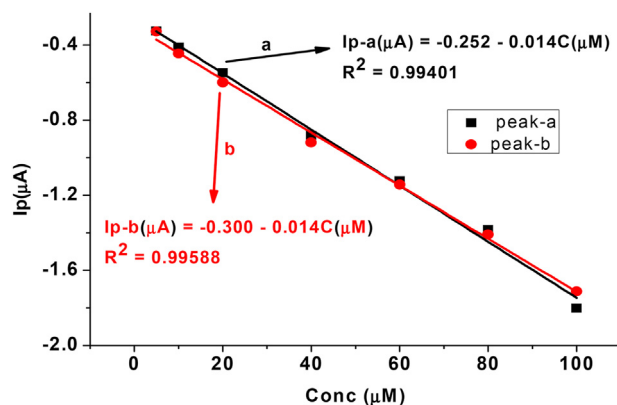recovery was investigated at 50, 100, and 200% of selected potential interferents (uric acid, ascorbic acid and ampicillin) (Figure 16). As can be seen from Table 2, detection of TC in capsule sample with a spike recovery result of 99.80%, and interference recovery results in the range 98.49 (for 200% of Amp) to 99.78% (for 50% of UA) indicated the reliability of the results and hence validated the applicability of the method for determination of TC in a real capsule formulation sample with a complex matrix.

3.8. Comparison of the present method with reported methods

The performance of the present method was compared with recently reported methods for determination of TC in terms of their linear dynamic range, and limit of detection parameters (Table 3). As can be seen from the table, the linear dynamic range of the present method (5–100 μM) is the second widest following the method using MWNT/COOH-GO/CPE [21], a
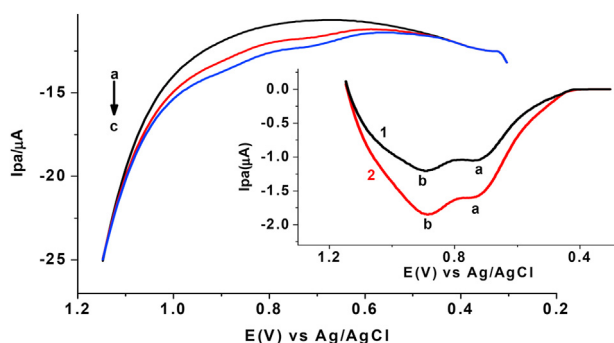
Figure 15. SWAdASVs of PMG/GCE in pH 7.5 PBS containing a) no, b) capsule sample claimed to be 56.98 μM, and c) b + 40 μM standard TC at E_{acc} 600 mV and t_{acc} 20 s. Inset: corrected for blank SWAdASVs for (1) unspiked capsule sample and (2) capsule sample spiked with 40 μM TC.

Figure 16. SWAdASVs of the capsule sample solution claimed to have 56.98 μM of TC in the presence of 28, 57, and 114 μM of Amp, AA, and UA in pH 7.5 PBS at PMG/GCE. E_{acc} 600 mV, and t_{acc} 20 s.

method which of course needs tedious electrode preparation. The method detection limit of the method is also the fourth lowest value following the methods that use carcinogenic Pb(II) [25], and expensive gold nanoparticle [23], and MWNT/GO [21]. Thus, the present method is an excellent candidate for determination of TC in real samples using a relatively cheap material following a one-step electrode modification procedure.

4. Conclusion

In this study, potentiodynamically fabricated poly(malachite green) modified glassy carbon electrode was characterized using cyclic voltammetry and electrochemical impedance spectroscopy using $[Fe(CN)_6]^{3-/4-}$ as a probe. Tetracycline showed two successive oxidative peaks with no peak in the reduction scan direction indicating irreversibility of the oxidation of tetracycline at the poly(malachite green)
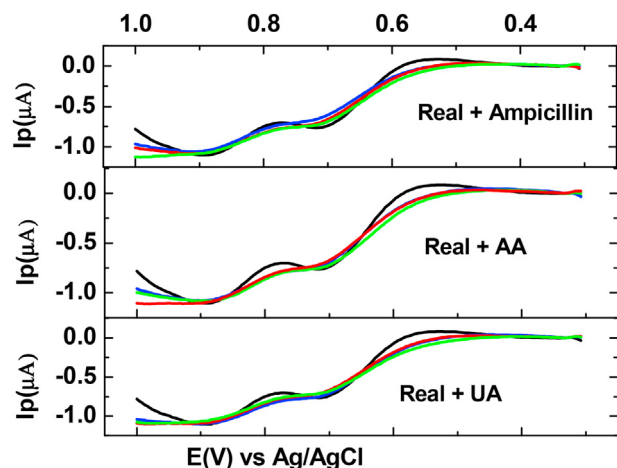
modified glassy carbon electrode. In contrast to the unmodified glassy carbon electrode, oxidative peaks with about threefold enhanced peak current at the poly(malachite green) modified glassy carbon electrode showed catalytic effect of the modifier towards tetracycline oxidation. While the observed peak potential shift with scan rate confirmed the irreversibility of the reaction, better correlation of the anodic peak current with scan rate than with square root of scan rate added to slope of 0.60 for plot of log peak current versus log scan rate confirmed that the reaction of tetracycline at the polymer modified electrode is predominantly adsorption controlled. The effect of experimental parameters such as accumulation potential, accumulation time and pH on the

Table 2. Summary of detected level of TC in the capsule sample solution, percent spike recovery, and interference recovery results of the method based on PMG/GCE.

Purpose of analysis	Sample analyzed	Spiked TC (μM)	Added interferent (μM)			Detected TC (μM)	Detected/Recovery (%)
			UA	AA	Amp		
TC in capsule sample	Capsule sample*	0	0	0	0	57.10	100.21
Spike recovery	Capsule sample*	40	0	0	0	96.79	99.80
Interference study	Capsule sample*	0	28	0	0	56.86	99.78
	Capsule sample*	0	57	0	0	56.66	99.44
	Capsule sample*	0	114	0	0	56.48	99.12
	Capsule sample*	0	0	28	0	56.75	99.60
	Capsule sample*	0	0	57	0	56.71	99.53
	Capsule sample*	0	0	114	0	56.66	99.44
	Capsule sample*	0	0	0	28	56.71	99.53
	Capsule sample*	0	0	0	57	56.66	99.44
	Capsule sample*	0	0	0	114	56.12	98.49

* capsule sample claimed 56.98 μM (according to labeled value); AA ascorbic acid; UA uric acid; Amp ampicillin.

Table 3. Comparison of the proposed method with selected recently reported methods for TC determination.

Electrode used	Method	Linear range (μM)	Detection limit (μM)	Ref.
MWNT/COOH-GO/CPE	DPSV	20–310	0.36	[20]
Graphite-polyurethane composite	DPV	3.8–38.0	2.6	[21]
AuNP/MWNT/GCE	DPV	11.25–315	0.09	[22]
Poly(Urethane)/CPE	DPV	3.8–19	2.6	[21]
PtNPs/C/GCE	DPV	9.99–44.01	4.28	[23]
Pb/poly(AP)/GCE	DPSV	0.05–10	0.004	[24]
Graphite-polyurethane composite	DPV	4.00–40.0	2.80	[25]
p-Mel@ERGO/GC	DPV	10–80	5.0	[26]
PMG/GCE	SWV	5–100	1.6	This work

electrochemical behavior of TC at PMG/GCE were evaluated. Detection of TC in capsule sample with an accuracy of 100.21% as claimed to be, spike recovery of 99.80%, and interference recovery in the range 98.49–99.78% in the presence of 50–200% of UA, AA, and Amp validated the reliability of the method. Compared to most of the recently reported methods for determination of TC, low limit of detection, and wide range of linear dynamic range of the present method make it an excellent potential candidate for determination of trace level of TC in real samples.

Declarations

Author contribution statement

Mahilet Turbale: Performed the experiments; Analyzed and interpreted the data; Wrote the paper.

Amsalu Moges, Mulugeta Dawit: Contributed reagents, materials, analysis tools or data.

Meareg Amare: Conceived and designed the experiments; Performed the experiments; Analyzed and interpreted the data; Contributed reagents, materials, analysis tools or data; Wrote the paper.

Data availability statement

Data will be made available on request.

Declaration of interests statement

The authors declare no conflict of interest.

Additional information

No additional information is available for this paper.

References

[1] F.F.G. Neto, R.S. Lima, W.S. Lyra, G. Marino, M.C.U. Araujo, E.P. Medeiros, V.B. Nascimento, Biamperometric determination of tetracycline in pharmaceuticals, Anal. Lett. 40 (16) (2007) 3070–3079.

[2] L.V. Faria, A.P. Lima, F.M. Araújo, T.P. Lisboa, M.A. Matos, R.A. Munoz, R.C. Matos, High-throughput amperometric determination of tetracycline residues in milk and quality control of pharmaceutical formulations: flow-injection versus batch-injection analysis, Anal. Methods 11 (41) (2019) 5328–5336.

[3] G.M. Eliopoulos, G.M. Eliopoulos, M.C. Roberts, Tetracycline therapy: update, Clin. Infect. Dis. 36 (4) (2003) 462–467.

[4] N. Wangfuengkanagul, W. Siangproh, O. Chailapakul, A flow injection method for the analysis of tetracycline antibiotics in pharmaceutical formulations using electrochemical detection at anodized boron-doped diamond thin film electrode, Talanta 64 (5) (2004) 1183–1188.

[5] D. Vega, L. Agüí, A. González-Cortés, P. Yáñez-Sedeño, J. Pingarrón, Voltammetry and amperometric detection of tetracyclines at multi-wall carbon nanotube modified electrodes, Anal. Bioanal. Chem. 389 (3) (2007) 951–958.

[6] X.-R. Jing, Y.-Y. Wang, W.-J. Liu, Y.-K. Wang, H. Jiang, Enhanced adsorption performance of tetracycline in aqueous solutions by methanol-modified biochar, Chem. Eng. J. 248 (2014) 168–174.

[7] Y. Levkovitz, D. Fenchel, Z. Kaplan, J. Zohar, H. Cohen, Early post-stressor intervention with minocycline, a second-generation tetracycline, attenuates post-traumatic stress response in an animal model of PTSD, Eur. Neuropsychopharmacol. 25 (1) (2015) 124–132.

[8] Y. Luo, J. Xu, Y. Li, H. Gao, J. Guo, F. Shen, C. Sun, A novel colorimetric aptasensor using cysteamine-stabilized gold nanoparticles as probe for rapid and specific detection of tetracycline in raw milk, Food Contr. 54 (2015) 7–15.

[9] M.P. Rodríguez, H.R. Pezza, L. Pezza, Ultrasound-assisted dispersive liquid–liquid microextraction of tetracycline drugs from egg supplements before flow injection analysis coupled to a liquid waveguide capillary cell, Anal. Bioanal. Chem. 408 (22) (2016) 6201–6211.

[10] S. Heta, I. Robo, The side effects of the most commonly used group of antibiotics in periodontal treatments, Med. Sci. 6 (1) (2018) 6.

[11] F.P. Vilela, C.N. Gomes, J. Passaglia, D.P. Rodrigues, R.G. Costa, M.R. Tiba Casas, S.A. Fernandes, J.P. Falcao, F. Campioni, Genotypic resistance to quinolone and tetracycline in Salmonella Dublin strains isolated from humans and animals in Brazil, Microb. Drug Resist. 25 (2) (2019) 143–151.

[12] P.B. Bookstaver, C.M. Bland, B. Griffin, K.R. Stover, L.S. Eiland, M. McLaughlin, A review of antibiotic use in pregnancy, Pharmacotherapy 35 (11) (2015) 1052–1062.

[13] H.Po. Tang, C. Ho, S.S.l. Lai, High-throughput screening for multi-class veterinary drug residues in animal muscle using liquid chromatography/tandem mass spectrometry with on-line solid-phase extraction, Rapid Commun. Mass Spectrom. 20 (17) (2006) 2565–2572.

[14] R. Althaus, M.I. Berruga, A. Montero, M. Roca, M.P. Molina, Evaluation of a microbiological multi-residue system on the detection of antibacterial substances in Ewe milk, Anal. Chim. Acta 632 (1) (2009) 156–162.

[15] I.D. Kargin, L.S. Sokolova, A.V. Pirogov, O.A. Shpigun, HPLC determination of tetracycline antibiotics in milk with post-column derivatization and fluorescence detection, Inorg. Mater. 52 (14) (2016) 1365–1369.

[16] A.R. Shalaby, N.A. Salama, S.H. Abou-Raya, W.H. Emara, F.M. Mehaya, Validation of HPLC method for determination of tetracycline residues in chicken meat and liver, Food Chem. 124 (2011) 1660–1666.

[17] S.A. Shama, A.S. El Sharkawy, A.H. Mahmoud, H.M. Hassan, S. > H. Nassar, Validation of modified HPLC method for determination of oxytetracycline, tetracycline and doxycycline in chicken meat and liver, N. Y. Sci. J. 9 (5) (2016) 68–74.

[18] K.I. Nikolaidou, V.F. Samanidou, I.N. Papadoyannis, Development and validation of an HPLC confirmatory method for the determination of seven tetracycline antibiotics residues in bovine and porcine muscle issues according to 2002/657/EC, J. Liq. Chromatogr. Relat. 31 (2008) 3032–3054.

[19] X. Dang, C. Hu, Y. Wei, W. Chen, S. Hu, Sensitivity improvement of the oxidation of tetracycline at acetylene black electrode in the presence of sodium dodecyl sulfate, Electroanalysis 16 (23) (2004) 1949–1955.

[20] A. Wong, M. Scontri, E.M. Materon, M.R. Lanza, M.D. Sotomayor, Development and application of an electrochemical sensor modified with multi-walled carbon nanotubes and graphene oxide for the sensitive and selective detection of tetracycline, J. Electroanal. Chem. 757 (2015) 250–257.

[21] C.M.F. Calixto, É.T.G. Cavalheiro, Determination of tetracyclines in bovine and human urine using a graphite-polyurethane composite electrode, Anal. Lett. 48 (9) (2015) 454–464.

[22] S. Palisoc, P.G. De Leon, A. Alzona, L. Racines, M. Natividad, Highly sensitive determination of tetracycline in chicken meat and eggs using AuNP/MWCNT-modified glassy carbon electrodes, Heliyon 5 (2019), e02147.

[23] R.T. Kushikawa, M.R. Silva, A.C.D. Angelo, M.F.S. Teixeira, Construction of an electrochemical sensing platform based on platinum nanoparticles supported on carbon for tetracycline determination, Sens. Actuators B Chem. 228 (2) (2016) 207–213.

[24] Z.R. Dizavandi, A. Aliakbar, M. Sheykhan, A novel Pb-poly aminophenol glassy carbon electrode for determination of tetracycline by adsorptive differential pulse cathodic stripping voltammetry, Electrochim. Acta 227 (2017) 345–356.

[25] C.M.F. Calixto, P. Cervini, É.T. Cavalheiro, Determination of tetracycline in environmental water samples at a graphite-polyurethane composite electrode, J. Braz. Chem. Soc. 23 (5) (2012) 938–943.

[26] S. Kesavan, D.R. Kumar, Y.R. Lee, J.-J. Shim, Determination of tetracycline in the presence of major interference in human urine samples using polymelamine/electrochemically reduced graphene oxide modified electrode, Sens. Actuators B Chem. 241 (2017) 455–465.

[27] M. Amare, S. Admassie, Potentiodynamic fabrication and characterization of poly(4-amino-3-hydroxynaphthalene sulfonic acid) modified glassy carbon electrode, J. Mater. Res. Technol. 9 (5) (2020) 11484–11496.

[28] Q. Wan, X. Wang, X. Wang, N. Yang, Poly (malachite green) film: electrosynthesis, characterization, and sensor application, Polymer 47 (22) (2006) 7684–7692.

[29] S.-M. Chen, J.-Y. Chen, R. Thangamuthu, Electrochemical preparation of poly(malachite green) film modified nafion-coated glassy carbon electrode and its electrocatalytic behavior towards NADH, dopamine and ascorbic acid, Electroanalysis 19 (14) (2007) 1531–1538.

[30] Y. Umasankar, A.P. Periasamy, S.-M. Chen, Electrocatalysis and simultaneous determination of catechol and quinol by poly(malachite green) coated multiwalled carbon nanotube film, Anal. Biochem. 411 (2011) 71–79.

[31] M. Xu, J. Zhu, H. Su, J. Dong, S. Ai, R. Li, Electrochemical determination of methyl parathion using poly(malachite green)/graphene nanosheets–nafion composite film-modified glassy carbon electrode, J. Appl. Electrochem. 42 (2012) 509–516.

[32] I.I. Suni, Impedance methods for electrochemical sensors using nanomaterials, Trac. Trends Anal. Chem. 27 (7) (2008) 604–611.

[33] L.J. Leeson, J.E. Krueger, R.A. Nash, Concerning the structural assignment of the second and third acidity constants of the tetracycline antibiotics, Tetrahedron Lett. 4 (18) (1963) 1155–1160.

[34] N.B. Swan, M.A. A Zaini, Adsorption of malachite green and Congo red dyes from water: recent progress and future outlook, Ecol. Chem. Eng. S 26 (1) (2019) 119–132.